JOURNAL OF VIROLOGY, Jan. 2010, p. 1066–1075 Vol. 84, No. 2
0022-538X/10/$12.00 doi:10.1128/JVI.01473-09

Mutations in the Ectodomain of Newcastle Disease Virus Fusion Protein Confer a Hemagglutinin-Neuraminidase-Independent Phenotype[▽]

Juan Ayllón, Enrique Villar, and Isabel Muñoz-Barroso*

Departamento de Bioquímica y Biología Molecular, Universidad de Salamanca, Edificio Departamental Lab 108/112, Plaza Doctores de la Reina s/n, 37007 Salamanca, Spain

Received 16 July 2009/Accepted 29 October 2009

The entry of enveloped viruses into host cells is preceded by membrane fusion, which in paramyxoviruses is triggered by the fusion (F) protein. Refolding of the F protein from a metastable conformation to a highly stable postfusion form is critical for the promotion of fusion, although the mechanism is still not well understood. Here we examined the effects of mutations of individual residues of the F protein of Newcastle disease virus, located at critical regions of the protein, such as the C terminus of the N-terminal heptad repeat (HRA) and the N terminus of the C-terminal heptad repeat (HRB). Seven of the mutants were expressed at the cell surface, showing differences in antibody reactivity in comparison with the F wild type. The N211A, L461A, I463A, and I463F mutants showed a hyperfusogenic phenotype both in syncytium and in dye transfer assays. The four mutants promoted fusion more efficiently at lower temperatures than the wild type did, meaning they probably had lower energy requirements for activation. Moreover, the N211A, I463A, and I463F mutants exhibited hemagglutinin-neuraminidase (HN)-independent activity when influenza virus hemagglutinin (HA) was coexpressed as an attachment protein. The data are discussed in terms of alterations of the refolding pathway and/or the stability of the prefusion and fusion conformations.

Newcastle disease virus (NDV) is an avian enveloped virus belonging to the family *Paramyxoviridae*. Two viral membrane-associated proteins are responsible for the entry of the virus into the host cell: they are hemagglutinin-neuraminidase (HN), a receptor-binding protein that interacts with sialoglycoconjugates at the cell surface, and F, a trimeric class I fusion protein that, upon activation, triggers the fusion of the viral and target membranes. F protein is activated after the attachment of its homotypic HN protein to the proper receptor; however, how HN activates F is not well understood. F protein is synthesized as an inactive precursor, F_0, that is activated by proteolytic cleavage to the disulfide-linked F_1-F_2 fusion-competent form (Fig. 1) (10). The crystal structures of several paramyxoviral fusion proteins, in both the prefusion and postfusion conformations (3, 26, 27), have revealed that these proteins undergo major conformational changes, from a metastable conformation to a highly stable, postfusion form. Several regions in the ectodomain of class I viral fusion proteins are involved in these conformational conversions, including a hydrophobic fusion peptide at the N terminus of the F1 protein and two hydrophobic heptad repeat motifs, HRA and HRB, located at its N and C termini, respectively (Fig. 1). In the prefusion form, HRB shows a triple-stranded coiled-coil conformation forming the stalk of the mushroom-like protein (3, 19, 27). Its globular head contains three domains, DI to DIII (Fig. 1), with the base of the head being formed by the DI and DII domains, with residues predominantly located between HRA and HRB. The top of the head is formed by DIII, consisting mainly of HRA and the fusion peptide, located on the side of the head sequestered between adjacent subunits. In this prefusion state, HRA is folded as two antiparallel β-strands and four (h1 to h4) helices (27) (see Fig. 6). The DIII domain undergoes major structural changes from the prefusion to the final postfusion conformation. HRA refolds as an α-helix, propelling the fusion peptide into the target membrane and generating a prehairpin intermediate (see Fig. 6). The final, stable conformation consists of a six-helical bundle (6HB), comprising a dimer of trimers in which the trimeric HRA coiled coil forms the core, packed along the outside by three antiparallel HRB α-helices (1, 3, 19, 27).

The refolding mechanism that triggers F protein activation is still not well understood. Mutational analysis of the HRA and HRB domains of paramyxovirus F proteins (3, 13, 18, 19, 22, 23), as well as the use of HRA- and HRB-derived peptides (6, 17), has led to the proposal of a series of discrete refolding intermediates of the F protein, from the metastable native conformation, through the prehairpin intermediate, and to the final postfusion hairpin structure (6HB) (17, 19, 27). To gain further insight into the individual residues critical for this mechanism, in this work we mutated several residues of the head and stalk of the NDV F protein (Fig. 1). The mutations disrupted F protein antibody reactivity, fusogenicity, and HN dependence in different ways. Interestingly, a mutant of the C-terminal h4 α-helix of HRA (N211A mutant) and two mutants of a residue located at the most N-terminal position of HRB (I463A and I463F mutants) exhibited a hyperfusogenic phenotype and HN-independent activity when influenza virus hemagglutinin (HA) was coexpressed as an attachment protein. The data are discussed in terms of alterations of the

* Corresponding author. Mailing address: Departamento de Bioquímica y Biología Molecular, Universidad de Salamanca, Edificio Departamental Lab. 112, Plaza Doctores de la Reina s/n, 37007 Salamanca, Spain. Phone: 34-923-294465. Fax: 34-923-294579. E-mail: imunbar@usal.es.

▽ Published ahead of print on 11 November 2009.

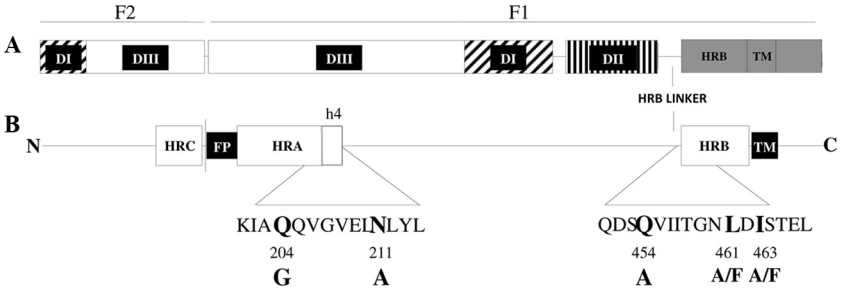

FIG. 1. Schematic representation of the structure of the NDV fusion protein. (A) Domain structure of F protein (27). (B) Locations of the fusion peptide, HR regions, and sequences studied. Mutated residues are indicated in bold.

refolding pathway and/or the stability of the prefusion and fusion conformations.

MATERIALS AND METHODS

Recombinant expression vectors and site-directed mutagenesis. pNDV/B1, which contains the full-length cDNA of the NDV Hitchner B1 strain (14), was used as a template for PCR amplification of the open reading frames (ORFs) of the *hn* and *f* genes. Primers were designed to incorporate new ClaI and BglII restriction sites at the 5′ and 3′ ends, respectively, of both the *hn* and *f* ORFs. PCR products were then cloned into the pGEM-T vector (Promega). Mutations in the *f* gene, which are shown in Fig. 1, were generated using a QuikChange site-directed mutagenesis kit (Stratagene) following the manufacturer's instructions, with pGEM-wild-type F as the template. Mutated products as well as wild-type *f* and *hn* were then subcloned between the ClaI-BglII sites of the mammalian pCAGGS expression vector (15). Multiple clones of each construct were verified by DNA sequencing. pCAGGS-mRFP, encoding the monomeric red fluorescent protein (2), and pCAGGS-SC/18 HA, encoding influenza virus strain A/South Carolina/1/18 hemagglutinin (9), were kindly provided by Adolfo García-Sastre.

Cell lines and transient expression systems. HeLa and BHK-21 cells, obtained from the American Type Culture Collection, were grown in Dulbecco's modified Eagle's medium (DMEM) supplemented with antibiotics and 10% fetal calf serum (FCS). Sixteen to 24 h prior to each experiment, cell monolayers at 80 to 90% confluence were transfected using Lipofectamine 2000 (Invitrogen) according to the manufacturer's instructions. All transfections were performed at a Lipofectamine-to-DNA ratio of 1:1. A total of 2 μg of plasmid DNA was used for each 35-mm tissue culture dish. The mixture of DNA and Lipofectamine in OptiMEM was incubated at room temperature and added to cells previously washed with OptiMEM. At 6 h posttransfection, the medium was replaced by DMEM containing 10% FCS and cells were incubated for 42 h at 37°C. In each experiment, pCAGGS-mRFP was used as a transfection control.

Quantification of cell surface expression by FACS analysis. Monolayers of HeLa cells transfected with 2 μg of plasmid DNA per 35-mm plate were collected and processed for fluorescence-activated cell sorting (FACS) as described before (7). Briefly, transfected cells were scraped from the plates, washed with phosphate-buffered saline (PBS), pelleted by centrifugation, and incubated for 15 min at room temperature in the presence of either 5 μg/ml monoclonal antibody (MAb) against NDV F (2A6 anti-F MAb) or 5 μg/ml anti-NDV rabbit serum, both generous gifts from Adolfo García-Sastre. After centrifugation, cells were resuspended in PBS and incubated with anti-mouse or anti-rabbit Alexa Fluor 488-conjugated IgGs (Invitrogen) for 15 min in the dark at room temperature, followed by incubation in FACS lysing solution (Becton Dickinson) for 10 min to fix and preserve the cells. Cells were then pelleted by centrifugation, washed with PBS, and resuspended in a suitable volume of PBS for analysis on a FACSCalibur flow cytometer (Becton Dickinson); at least 10^5 cells were measured. Mean fluorescence values and the % cells with fluorescence higher than the background were combined to quantify expression and were normalized to the values for the NDV wild-type F protein.

Immunofluorescence. Monolayers of HeLa cells in 24-well plates were transfected with 1 μg of plasmid per well. At 16 h posttransfection, cells were fixed for 30 min in PBS containing 2.5% paraformaldehyde, blocked for 1 h in PBS containing 1% bovine serum albumin (BSA), and incubated for 1 h at room temperature with 5 μg/ml of 2A6 anti-F5 MAb or 5 μg/ml rabbit polyclonal antibody (PAb) against NDV. Cells were then incubated with anti-mouse or anti-rabbit Alexa Fluor 488-conjugated IgGs for 45 min and visualized under an inverted fluorescence microscope (Olympus IX51) at a magnification of ×10.

Syncytium assays. Monolayers of HeLa or BHK-21 cells grown in 12-well plates were cotransfected with 1 μg pCAGGS encoding different F mutants and with either HN, HA, or empty pCAGGS, for a total amount of 2 μg of DNA per well. At 24 h posttransfection, cells were washed and F protein was activated by digestion with acetyl trypsin as described previously (20). Fresh medium was then added, and the cells were incubated at 37°C for different times, after which they were fixed with 10% formaldehyde and stained with crystal violet for syncytium observation. Representative fields were captured with an inverted microscope (Olympus IX51). Quantification of syncytia was accomplished by measuring the area in pixels, referring to the total area of the field for three random fields. Areas were quantified using the analysis tool in Adobe Photoshop CS4.

Dye transfer assays for lipid and aqueous content mixing. To measure whether any of the NDV F mutants were deficient in either lipid mixing or content mixing, as well as their HN and temperature dependence, a standard dye transfer fusion assay was performed. Human erythrocytes (RBCs) were double labeled with calcein and octadecyl rhodamine B chloride (R18) (both from Molecular Probes). Briefly, RBCs at 10% hematocrit in PBS were incubated with 100 μg/ml of the aqueous dye calcein for 1 h at 37°C in the dark. After extensive washing, RBCs were collected by centrifugation and incubated with 50 μg/ml of the lipid probe R18 for 30 min at room temperature in the dark, followed by several washing steps to remove unincorporated dye from labeled cells. Monolayers of HeLa cells in 12-well plates were transfected as described above. At 16 h posttransfection, F protein was activated as described above, and cells were overlaid with 250 μg of DMEM with dye-labeled RBCs at 0.2% hematocrit per well. The effector-target cell complexes were incubated at different temperatures and times, depending on the experiment. Nuclei were stained by incubation with 10 μg/ml of Hoechst dye. Cells then were washed several times with PBS to remove unbound RBCs, and dye transfer was visualized under an inverted fluorescence microscope at a magnification of ×10. The extent of fusion was calculated as the percentage of dye-labeled cells in the total number of nuclei and was normalized to the value obtained with wild-type F- and HN-expressing cells at 37°C.

RESULTS

Construction and expression of mutant proteins. In consideration of the crystal structures of the NDV and parainfluenza virus 5 (PIV5) F proteins (3, 27), several residues located on the head and stalk of the NDV F protein were mutated. In the extended HRA domain observed in the postfusion conformation of the NDV F crystal (3), the side chains of Q204, V208, and N211 form a cavity. This cavity might be involved in interactions that stabilize the DIII domain (Fig. 1) or in the structural changes that DIII undergoes from the prefusion stage to the fusion conformation (27). Furthermore, Q204 and N211 correspond to heptad repeat residues when aligned with the PIV5 protein (27). Thus, Q204 aligns with PIV5 A190 and N211 and with PIV5 N197, with both areas being part of the putative h4 region at the C terminus of HRA (27). This region

TABLE 1. Surface expression of mutant F proteins and MAb 2A6 reactivity

Mutant	% Positive events (mean ± SD)[a]	
	PAb	MAb 2A6
Q204G	102.603 ± 34.5	96.738 ± 20.2
N211A	186.559 ± 41.1	65.152 ± 19.7
Q454A	97.364 ± 29.6	83.899 ± 20.7
L461A	126.213 ± 21.0	93.409 ± 12.2
L461F	101.261 ± 28.1	98.869 ± 23.6
I463A	167.048 ± 8.6	42.111 ± 10.1
I463F	155.560 ± 16.6	78.060 ± 25.0

[a] Values were calculated as geometric means multiplied by the percentage of positive events (% of cells with higher fluorescence than that of controls) and were normalized to the value for NDV wild-type F. Data are means ± SD for three independent experiments.

remains as a helical domain in both the prefusion and postfusion states and remains in close proximity to the HRC of F_2 in both. Accordingly, to analyze the role of this region, Q204 and N211 were replaced by G and A, respectively. These changes modified the size and polarity of the residues to change the amino acid pattern that affords the heptad repeat its structural properties.

In the crystal structure, residues Q445 to Q454 emerge from the neck region of the NDV fusion protein to enter the groove of the HRA coiled coil immediately below the N terminus of the F_2 HRC domain (3). These residues belong to the HRB linker, which interacts with the newly exposed DIII domain at the neck of the protein in the PIV5 postfusion conformation (Fig. 1) (27). In the prefusion conformation of the PIV5 F protein described by Yin et al. (27), the HRB linker shows weak electron density, suggesting flexibility. To further analyze the role of this region, NDV F Q454, which aligns with SV5 F Q440, was mutated to A.

In the PIV5 F protein, amino acids L447 and I449, located in the N-terminal region of HRB, have been shown to play an important role both in fusion activation and in the stabilization of the postfusion six-helix-bundle structure (18). We aimed to study the role of these residues in a related paramyxovirus, namely, NDV. Thus, the corresponding amino acids, L461 and I463, were replaced by A or F.

Cell surface expression levels of the mutant proteins were analyzed by FACS analysis and by immunofluorescence. The results of cell surface expression analysis differed, depending on the antibodies used to recognize the protein. Four of the mutants (Q454A, L461A, L461F, and Q204G) showed similar cell surface expression levels or slightly lower ones than that of the wild-type F protein when probed with both monoclonal anti-F 2A6 and polyclonal antibodies (Table 1). These four mutants, as well as the wild-type F protein, were also better recognized by the MAb in the immunofluorescence assays (data not shown). Another three mutants (L463A, I463F, and N211A) reacted mainly with the PAb, apparently showing significantly higher surface expression levels than those of the wild type (Table 1). Nevertheless, when these three mutants were probed with the MAb, the data were the opposite, indicating lower reactivities (Table 1). Considering the polyclonal reactivity of the mutant proteins, it is possible that the I463A, I463F, and N211A mutants could be expressed at higher levels than those of the wild type, whereas the Q454A, L461A, L461F, and Q204G mutants were expressed at similar levels. According to our results, the MAb 2A6 might be a conformation-specific antibody that better recognizes the wild-type conformation; therefore, we could be detecting a conformational change in the F protein resulting from the I463A, I463F, and N211A mutations, as the epitope recognized by the MAb may be exposed better in wild-type F. In light of its failure to bind to wild-type F in Western blot and immunoprecipitation assays (data not shown), this antibody seems to be conformation dependent. Taken together, our flow cytometry and immunofluorescence studies suggested that all of the mutated proteins were expressed at the cell surface. Owing to the lack of an appropriate antibody for immunoprecipitation assays, we failed to analyze whether the cell surface-expressed proteins were properly processed, i.e., whether they had undergone similar posttranslational modifications and whether they were proteolytically activated in a similar proportion to that of the wild type.

Effects of mutations on cell-cell fusion. To examine the ability of the different F mutant proteins to promote cell-cell fusion, both syncytium and dye transfer assays were performed. Data from a representative experiment showing syncytium formation on F-transfected HeLa cells cotransfected with HN (+HN) or with HA (−HN) are shown in Fig. 2. Similar results were obtained on transfected BHK-21 cells (data not shown). Syncytia were quantified by measuring the covered areas in three random fields and referring these to the total area in the field (Table 2). With the exception of the Q454A mutant, all of the mutants promoted syncytium formation in the presence of HN coexpression. Five of the mutants, the N221A, L461A, L461F, I463A, and I463F mutants, increased the extent of syncytium formation in comparison with wild-type F protein. Furthermore, the I463A, I463F, and N211A mutants caused extensive syncytium formation in the absence of HN coexpression.

To further quantify the extent of cell-cell fusion, we performed a dye transfer assay in the presence of HN cotransfection (Fig. 3A and B). Transfer of the lipophilic probe R18 from the membranes of RBCs to effector cells indicates lipid mixing or hemifusion, whereas transfer of the aqueous dye calcein is a measure of the mixing of cytoplasmic contents. These results confirmed those of the syncytium assays (Fig. 2; Table 2): the Q454A mutant was not able to promote either lipid or aqueous probe transfer, and it did not exhibit a hemifusion phenotype. The Q204G mutant, which was expressed on the cell surface at similar levels to those of wild-type F protein, promoted fusion to a slightly lesser extent than the wild type did. The N211A, L461, and I463 mutants exhibited greater extents of dye transfer, with no differences in lipid mixing or aqueous mixing (Fig. 3A and B). Fusion enhancement, determined by mutations in L461, was greater when L was replaced by A, whereas the most fusogenic phenotype was observed when I463 was modified by the aromatic residue F. The N211A, I463A, and I463F mutants showed higher cell surface expression levels than the wild type when probed with the polyclonal antibody (Table 1). It has previously been reported that cell-cell fusion activity is directly dependent on cell surface protein expression (5). Thus, to check whether the high fusogenicity levels of these mutants were due to enhanced expression, additional R18 dye transfer

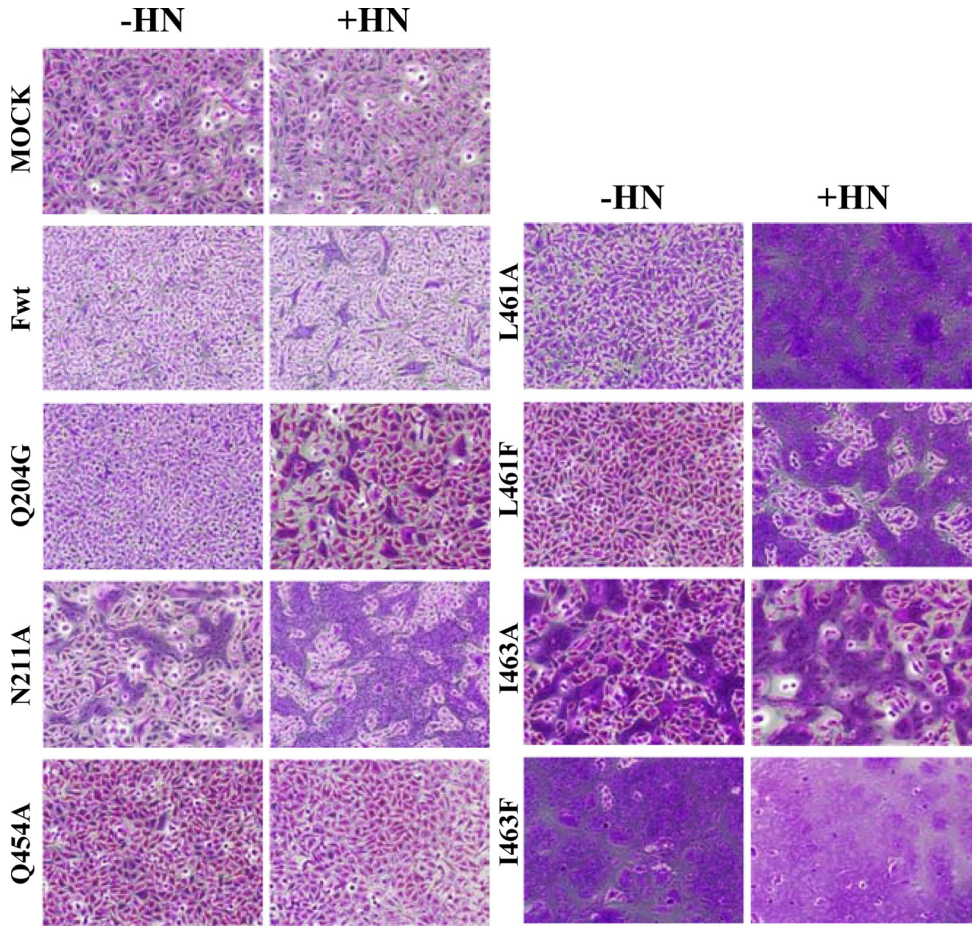

FIG. 2. Syncytium assay of cell-cell fusion. HeLa cells expressing wild-type F or F mutants cotransfected with NDV HN (+HN) or HA (−HN) in the presence or absence of HN were treated with acetyl trypsin for activation of F_0 precursors, and at 3 h postactivation, the cells were fixed and stained with crystal violet for syncytium observation. No syncytia were observed in unactivated replicates (data not shown). Representative photomicrographs are shown.

assays were performed to analyze the effect of decreasing amounts of transfected DNA. HeLa cells were transfected with 1 μg of HN and various amounts of F DNA. The extent of fusion was measured as the % of R18-labeled cells. The results shown in Fig. 3C indicate that hyperfusogenicity was maintained with decreasing levels of expression, whereas dye transfer induced by wild-type F was dependent on the DNA concentration (Fig. 3D). As a control for the effectiveness of transfection, pCAGGS encoding the monomeric red fluorescent protein (mRFP) was transfected. The data summarized in Fig. 3D show that the expression of mRFP was dependent on the DNA concentration. Accordingly, it could be inferred that this would be the case for mutant and wild-type F proteins.

TABLE 2. Quantification of syncytia produced by F protein mutants

Mutant	% Area per field[a]			
	HeLa cells		BHK-21 cells	
	−HN	+HN	−HN	+HN
Wild type	ND	32 ± 16.7	ND	6.5 ± 2.3
Q204G	ND	29.5 ± 13.4	ND	5.2 ± 1.1
N211A	34.7 ± 1.5	74.5 ± 15.2	9.2 ± 1.3	23.2 ± 1.7
Q454A	ND	ND	ND	ND
L461A	1.1 ± 0.9	89.6 ± 18.0	ND	62.8 ± 14.3
L461F	ND	60.8 ± 3.6	ND	9.9 ± 1.9
I463A	19.7 ± 11.2	65.3 ± 6.9	13.4 ± 2.5	21.9 ± 5.3
I463F	88.4 ± 4.6	99.0 ± 1.7	26.4 ± 7.4	62.8 ± 12.2

[a] Values were calculated by measuring the area covered by syncytia and referring it to the total area of the field. Data are means ± SD for three random fields. ND, not detected.

Fusion activity of the hyperfusogenic I463A, I463F, and N211A mutants. The dependence on HN of the hyperfusogenic I463A, I463F, and N211A mutant proteins for cell-cell fusion was analyzed in dye transfer assays. To study fusion in the absence of HN coexpression, the F mutants were also coexpressed with the influenza virus HA protein, acting as a nonhomotypic receptor-binding protein. This protein activates fusion at acidic pH, and therefore, under our experimental conditions at neutral pH, no fusion due to HA was detected (data not shown). No dye transfer was observed in the absence of an attachment protein (influenza virus HA or NDV HN) either in the wild type or in any mutant (data not shown). As shown in Fig. 4A, the I463A, I463F, and N211A mutant proteins exhibited extensive cell-cell fusion in the absence of HN

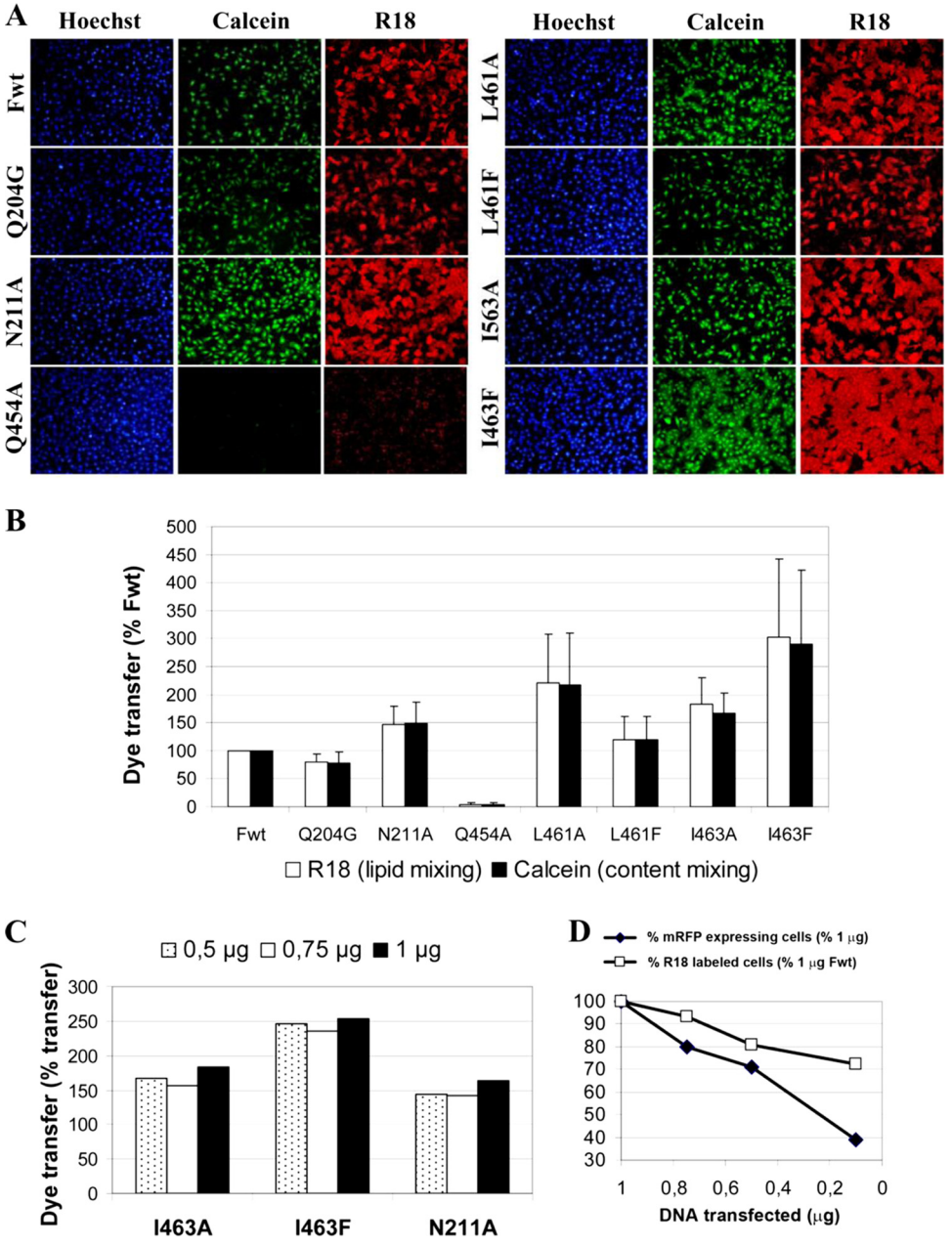

FIG. 3. Dye transfer assays of cell-cell fusion. Effector HeLa cells coexpressing F mutant and HN proteins were overlaid with RBCs labeled with both lipophilic R18 (red) and aqueous calcein (green), as described in Materials and Methods, and were incubated for 30 min at 37°C. (A) Photomicrographs from a representative experiment. (B) Quantification of lipid and content mixing. Combined results ± standard deviations (SD) for triplicate experiments are shown. The % of cells labeled with either R18 or calcein was calculated for three random fields in each experiment and related to that of wild-type F. (C) Dose-response study of dye transfer promoted by the I463A, I463F, and N211A mutants. Cells were transfected with 1 μg of HN and 0.5 μg, 0.75 μg, and 1 μg of F DNA. (D) Dose-response study of mRFP expression (◆) and R18 transfer of wild-type F (□) under the control of the CAGGS promoter. HeLa cells were transfected with different amounts of pCAGGS-mRFP or pCAGGS-wild-type F plus 1 μg of pCAGGS-HN. For the quantification of mRFP expression, at 16 h posttransfection cells were fixed with paraformaldehyde and nuclei were stained with Hoechst dye. Three random fields for each DNA concentration were photographed, and the % of mRFP-expressing cells was determined and related to that of cells transfected with 1 μg pCAGGS-mRFP. Wild-type F fusion promotion was analyzed in R18 transfer assays as described above. Results were related to those of cells transfected with 1 μg of pCAGGS-wild-type F. Data are means from duplicate experiments.

coexpression, as in the syncytium experiments (Fig. 2; Table 2). Both probes, calcein and R18, were transferred from RBCs to F-expressing cells, with similar efficiencies. High levels of hemadsorption due to HA were seen on the wild-type F-R18 field without probe transfer, probably due to the lack of neuraminidase activity in influenza virus HA.

To further analyze the homotypic HN dependence of the three mutant proteins, the time dependence of fusion in

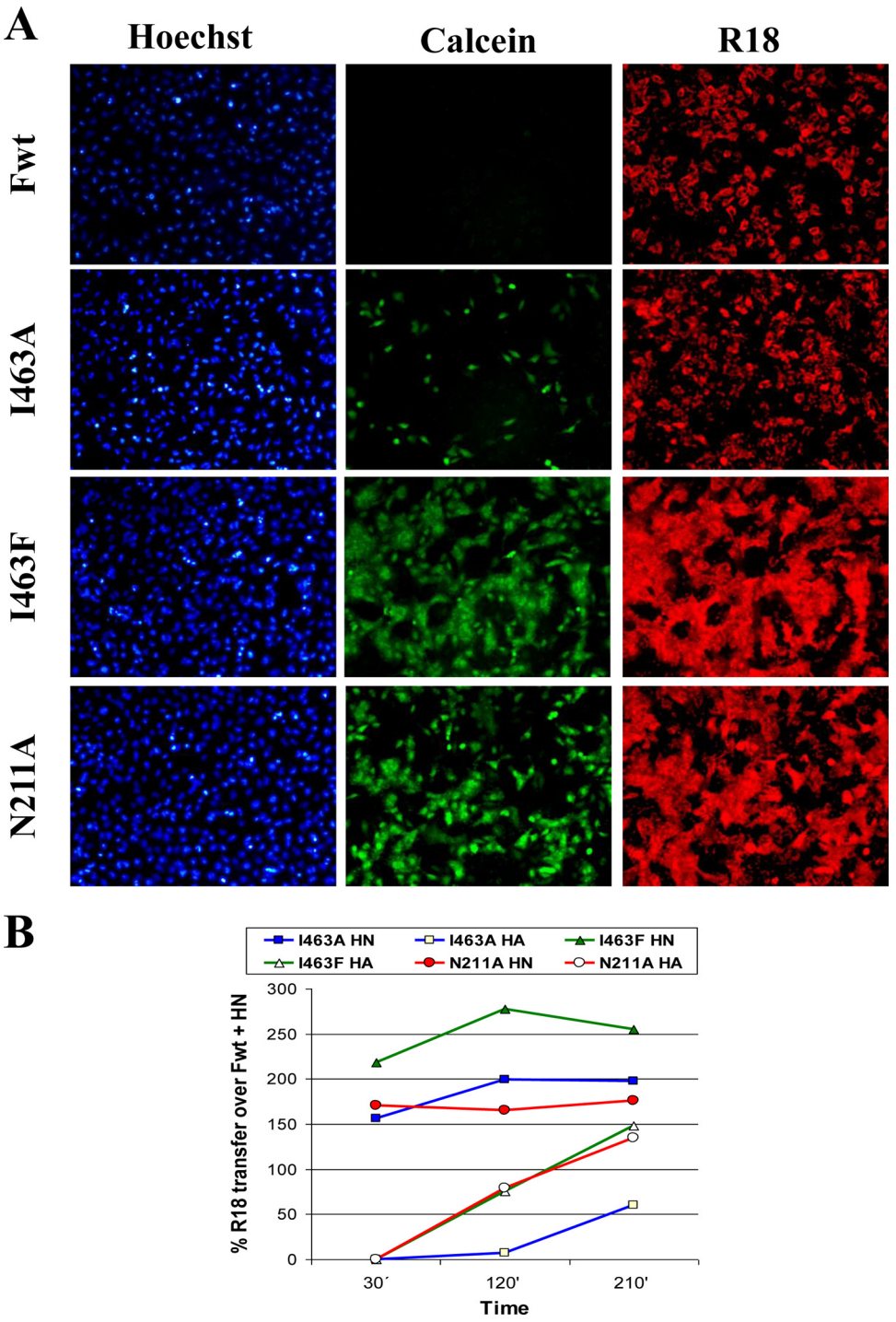

FIG. 4. Fusion activity of I463A, I463F, and N211A mutants in the presence or absence of HN protein expression. Effector HeLa cells were cotransfected with mutant F- and HA-expressing pCAGGS as detailed in Materials and Methods. RBCs labeled with both R18 (red) and calcein (green) were then added. (A) Representative fields of HeLa cells coexpressing influenza virus HA and F mutants 210 min after being overlaid with R18/calcein-labeled RBCs. High levels of hemadsorption due to HA can be seen on the wild-type F-R18 field without probe transfer. (B) Time dependence of dye transfer (R18) in the presence or absence of HN. Data are means for triplicate experiments.

the presence or absence of HN was analyzed by quantifying the extent of transfer of R18 from RBCs to transfected cells (Fig. 4B). The hyperfusogenic phenotype of the three mutants was maintained in the presence of HN at the three times assayed. At the longest time assayed (210 min), the three mutants induced cell-cell fusion in the absence of HN. Nevertheless, fusion was slower in the absence of the NDV homotypic attachment protein, with no detection of dye transfer at 30 min

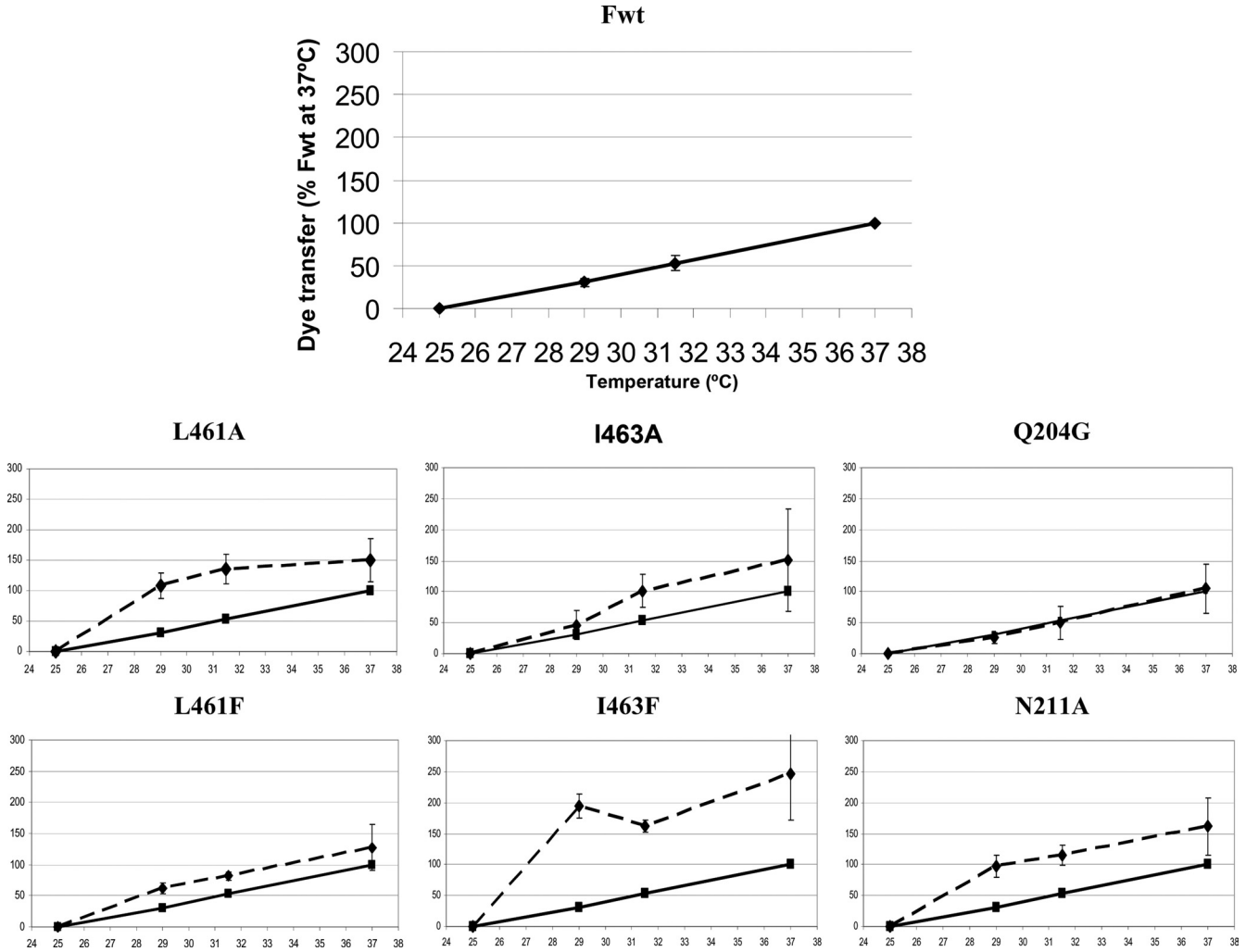

FIG. 5. Temperature dependence of fusion promoted by F mutants. RBCs were double labeled with R18 and calcein as described in Materials and Methods. HeLa cells expressing HN and F mutants were incubated with labeled RBCs (0.2% hematocrit) at different temperatures for 30 min. After washing of unbound RBCs, the extent of dye transfer was analyzed and referred to that of wild-type F at 37°C. Data concerning calcein transfer are shown and are similar to those for R18 transfer. Results are means ± SD for three independent experiments. Solid lines, wild-type F; dashed lines, F mutants.

for effector-target cell cultures of any of the mutants. The I463A mutant proved to be the one most dependent on HN; only after 210 min of incubation did we detect about 50% of the wild-type fusion level, although in the presence of HN, fusion induced by this mutant was about 200% greater than that observed in the controls (Fig. 4B). At the longest time assayed, the N211A mutant induced cell-cell fusion at levels slightly lower than those observed in the presence of homotypic HN. In the absence of HN, the I463F mutant, the most fusogenic mutant in the presence of homotypic HN, showed similar behavior to that of the N211A mutant.

Temperature dependence of mutant F proteins. It has been proposed that some mutant F proteins show a decrease in the energy barrier needed for protein activation prior to the triggering of fusion (16). To analyze whether the hyperfusogenic phenotype shown by some of the mutants analyzed in this work was due to an alteration in the energy threshold for fusion activation, the fusion activity of mutant proteins was studied at different temperatures and compared to that of wild-type F. We analyzed the fusion activity of mutant proteins as a function of the incubation temperature. To accomplish this, dye transfer fusion assays were performed as described above; R18- and calcein-double-labeled RBCs were bound to HeLa cells expressing HN and one mutant F protein, and the target-effector complexes were incubated for 30 min at 25°C, 29°C, 31.5°C, and 37°C. Figure 5 shows the extents of content mixing (calcein); the extents of lipid mixing (R18) were similar (data no shown). The results were referred to those of wild-type F at 37°C. All proteins except the Q454A mutant promoted membrane fusion at temperatures above 25°C, with no dye transfer observed at 25°C for any of the mutant proteins or the wild type. The fusion activity of the wild-type F protein fell to 53% efficiency at 31.5°C and to 30% at 29°C, similar to the results observed for the Q204G mutant; the other five mutants, the N211A, L461A, L461F, I463A, and I463F mutants, maintained their hyperfusogenic phenotype at the three fusion-permissive

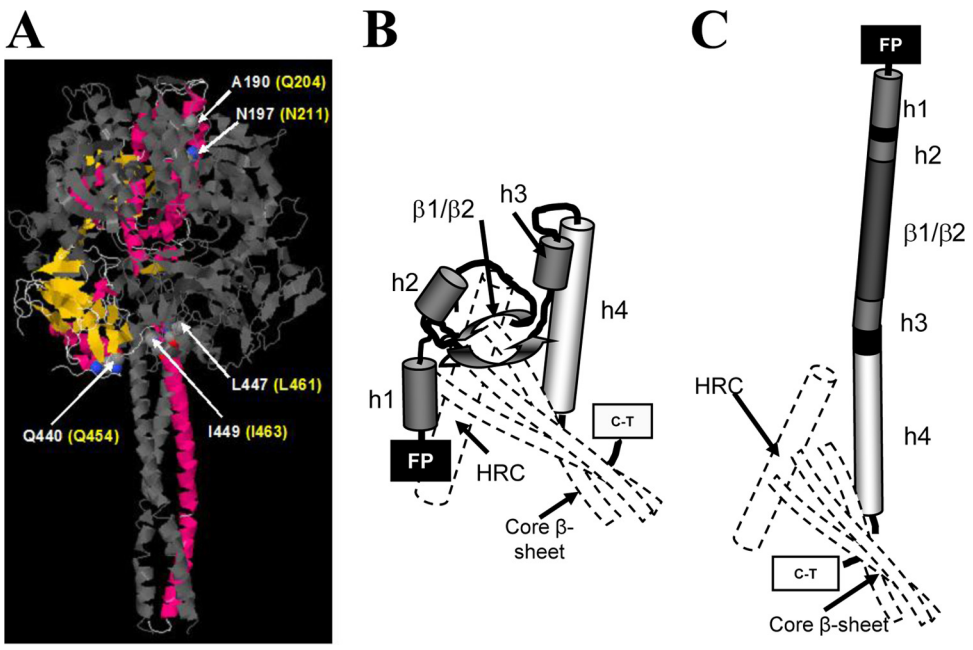

FIG. 6. Scheme of conformational changes in HRA from prefusion to postfusion state. (A) Ribbon model of PIV5 F protein in its metastable prefusion conformation (PDB accession number 2b9b) (27), showing some residues (named in white) from the A subunit and the corresponding residues in the NDV F protein (named in yellow). Subunits B and C are depicted in gray for clarity. (B) In the metastable, prefusion conformation, HRA is folded as a spring-loaded mixture of α-helices, turns, and β-strands, comprising 11 segments in the DIII head domain of the trimer (27). (C) After fusion, HRA is presented as a single long helix that allows the fusion peptide to be buried in the target membrane. The approximate positions of HRC and the core β-sheet are shown as dashed lines for both conformations.

temperatures of 29°C, 31.5°C, and 37°C compared with the wild type. At 29°C, the N211A and L461A mutants promoted similar dye transfer levels to those of the wild type at 37°C, with those of the I463F protein being significantly higher at this temperature. Although the transfection efficiency of I463F mutant-encoding DNA was less than 100% (data not shown), most of the cells were stained with both dyes at the lower temperature (29°C) due to the extensive syncytium formation promoted by this hyperfusogenic mutation. The results concerning temperature dependence proved to be different for the I463 and L461 mutants. When I463 was mutated to an aliphatic A residue, the mutant protein also showed hyperfusogenic activity at the three temperatures assayed, but to a reduced extent in comparison with that of the I463F mutant. Nevertheless, the replacement of L461 by the aromatic F residue afforded a slightly more fusogenic protein than the wild type, whereas the L461A mutant was hyperfusogenic at all three temperatures assayed, although to a lesser extent than the I463F mutant. Despite the lower temperature threshold (Fig. 5), the syncytium formation (Fig. 2; Table 2) and dye transfer ability (Fig. 3A and B) of the L461A mutant were comparable to those of other hyperfusogenic mutants (N211A and I463F), but the L461A mutant was unable to escape the requirement of HN (Fig. 2). According to its syncytium promotion and dye transfer abilities, the Q204G mutant showed a similar temperature dependence to that of wild-type F. To test whether the fusion promotion impairment of the Q454A mutant could be reversed at elevated temperatures, we performed dye transfer fusion assays at 45°C. No R18 or calcein transfer was observed (data not shown). In sum, these data suggest that the N211A, L461A, I463A, and I463F mutations could alter the structure of the protein, leading it to be less stable and hence determining a lower activation energy for the conformational changes that trigger membrane fusion.

DISCUSSION

The entry of enveloped viruses into the host cell is preceded by membrane fusion, which in paramyxoviruses is triggered by the F protein. Upon activation, this protein undergoes major irreversible conformational changes, from a metastable prefusion state to a highly stable postfusion hairpin structure. According to structural and biochemical data (17, 19, 27), the F refolding pathway consists of different discrete steps: first, melting of the stalk HRB coiled coil; second, formation of the HRA coiled coil, which pulls the fusion peptide toward the target membrane (prehairpin intermediate); and third, formation of the final hairpin structure of 6HB, which allows membrane juxtaposition and merging. In this pathway, different regions of the F ectodomain undergo major rearrangements. Several studies have revealed the importance of individual residues of HRA and HRB in the folding and functionality of paramyxovirus fusion proteins (3, 12, 13, 18, 22, 23). Additionally, other residues in the ectodomain of the F protein might be involved in structural stabilization of the protein and/or in the refolding mechanism. To assess the importance of particular amino acids in F functionality, we performed directed mutagenesis of several residues in the sequence of the NDV F ectodomain. In the prefusion conformation, HRA is broken into 11 segments, consisting of α-helices (h1 to h4), β-strands, and turns (27) (Fig. 6). We first focused our attention on residues in the C-terminal h4 helix of HRA. Amino acids Q204

and N211, which are heptad repeat residues located closest to the C terminus of h4, were both replaced by neutral aliphatic amino acids: the Q204G mutant showed a similar antibody reactivity and HN requirement to those of the wild type and promoted similar or slightly lower levels of membrane fusion. In contrast, the N211A mutant showed differences in antibody reactivity with respect to the wild type (Table 1), suggesting an alteration in the metastable form of the protein. Additionally, the N211A mutant showed a hyperfusogenic phenotype at all permissive fusion temperatures assayed (Fig. 2, 3, and 5) and exhibited HN-independent fusion activity when HA was coexpressed as the attachment protein. The coexpression of HN enhanced the fusion kinetics, although the N211A and wild-type proteins promoted similar fusion levels at longer times (Fig. 4). Together, these data seem to indicate a major effect of N replacement by A at position 211 on the functionality of the F protein, decreasing the energy barrier for the proper conformational changes to occur even in the absence of HN protein. Several nonexclusive possibilities could be invoked to explain the reported effects of the N211A mutant protein: (i) N211 is a key residue in the stabilization of the prefusion conformation, (ii) N211 is a key residue in the assembly of HRA leading to the fusion stage (Fig. 6), and (iii) N211 is a key residue in the interaction with HN. Based on comparison of the crystal structures of both the prefusion and postfusion conformations of paramyxovirus F proteins (27), it has been proposed that polar residues at the h4 HRA might be involved in the regulation of packing changes between the pre- and postfusion forms. Our data support this hypothesis and suggest that replacing the polar N211 with the nonpolar and small A would disturb key interactions established by the C terminus of h4, destabilizing the prefusion DIII domain and facilitating the functional refolding of F protein even in the absence of HN protein. In the crystal structures, the h4 C-terminal helix of HRA remains in close proximity to F_2 HRC in both the prefusion and postfusion conformations (3, 27) (Fig. 6), packing the N-terminal half of the HRC helix in a parallel fashion into the groove of the HRA coiled coil (3). In this context, replacing the polar N residue by a nonpolar and small A residue would alter stabilizing h4-HRC interactions and thus facilitate F protein refolding. Previous mutagenesis studies of paramyxovirus F HRA have focused on residues located in the more N-terminal regions of HRA (12, 22, 23, 25). Most of the resulting proteins were fusion deficient, while others enhanced fusion. According to the available structural data (27), the N-terminal segments of HRA would undergo major rearrangements, leading to HRA extension. The fusion-inhibitory mutations in this region would block such rearrangements, preventing the triggering of fusion, while enhancing mutations would act by destabilizing the prefusion HRA, as we propose for the N211A mutation. Nevertheless, to our knowledge, none of these mutations has been reported to overcome the requirement of homotypic HN coexpression, as in the case of the N211A mutant. Interestingly, a hyperfusogenic mutation, L289A, has been reported for the NDV F protein, and it did not require HN for fusion in COS-7 cells (21) and enhanced fusion in an HN-dependent manner in BHK cells (11). Residue L289 is located in the central strand of the β-sheet that constitutes the DIII core, together with HRA h4 and HRC (3, 27) (Fig. 6). This structure might serve as the platform for HRA rearrangements and would be disrupted by the N211A and L289A mutations, leading to the destabilization of the protein and triggering the refolding pathway.

In the C-terminal region of the postfusion NDV F ectodomain, segment Q445-Q454 emerges from the DII domain to enter the groove of the HRA coiled coil immediately below the N terminus of HRC (3). The paramyxovirus HRB linker (residues 422 to 445 in PIV5, corresponding to residues 435 to 459 in NDV) has been suggested to be a flexible region (1) that might be crucial in the first step of the proposed F refolding pathway, consisting of the melting of HRB helices to open the HRB stalk (27). In our work, residue Q454, which aligns with Q440 of PIV5, was replaced by A. Showing similar antibody reactivity to that of the wild type (Table 1), mutant proteins were expressed at the cell surface, but they were not able to trigger either complete fusion or hemifusion even when the temperature was raised to 45°C (data not shown). As a consequence of the replacement of a polar Q residue by a smaller, hydrophobic A residue, key interactions in the prefusion form of the protein might be altered. In PIV5, the replacement of S443 (three residues upstream from the corresponding Q454, i.e., Q440) by proline resulted in a hyperfusogenic protein that was functional in the absence of HN (16). The hyperfusogenic S443P mutation has a destabilizing effect on F protein, with the mutant being expressed in its postfusion conformation (4). In the crystal, S443 forms hydrogen bonds with D445 in the prefusion conformation (27), and it has been described as being important for stabilizing the prefusion conformation. In the present work, the absence of fusion promotion by the Q440A mutant might involve an important modification of HRB linker flexibility, resulting in the prevention of the proper conformational changes of F from the first step. Another possibility is that the linker might act as a structural inhibitor in the prefusion conformation to prevent the triggering of F in the absence of the target cell. If this were the case, then the Q454A mutant might alter the prefusion conformation, allowing the protein to acquire the postfusion state in the absence of the target cell and thus to become inactivated. Finally, the mutation could also stabilize the prefusion state, increasing the energy threshold required for fusion to be triggered, although high temperatures do not reverse the nonfusion phenotype.

Finally, our data on the mutations of amino acids L461 and I463, located at the most N-terminal position of HRB (Fig. 6), confirmed their key role in the functionality of paramyxovirus fusion proteins, as proposed previously (18). These residues contribute to the network of intersubunit interactions at the base of the head of the trimer, stabilizing the prefusion conformation of F (27). In PIV5, mutations of the corresponding L447 and I449 residues to aromatic, but not aliphatic, residues destabilized the prefusion F conformation, suggesting a key role in the regulation of the conformational changes between the native and the fusogenic conformation (18). Nevertheless, our data (Fig. 2 to 5) showed that in NDV F, replacements of residues L461 and I463 by aliphatic A or aromatic F resulted in hyperfusogenic proteins. At lower temperatures, the mutants promoted fusion more efficiently than the wild type, meaning that they had lower energy requirements for activation. Additionally, our data showed a greater effect on F functionality when L461 was replaced by A. These different results with respect to previously reported data may imply differences be-

tween viruses or may also be due to the mutant PIV5 strain used by Russell et al. (18) (W3A), whose F protein is able to fuse in the absence of HN. According to our data, only the two substitutions of I463 escaped the HN requirement for fusion, showing that hyperfusion activity may not be related to the HN requirement. This conclusion is supported by the observed differences in antibody reactivity, which was similar to that of the wild type for L461 mutants but different for I463 mutants as well as for the other HN-escaping mutant, the N211A mutant, as discussed above. The crystallographic data on the prefusion PIV5 F protein show a central position for the three residues corresponding to I463 at the base of the head of the trimer (27). Our results point to the critical role of this residue in F functionality.

In sum, several individual residues located in different protein segments have been shown to be critical for the activation mechanism of NDV F. Some of the mutants proved to be highly fusogenic proteins that could be used to enhance the therapeutic potential of recombinant NDV vectors, since F-protein-induced syncytium formation has been reported to be an important mechanism in NDV oncolysis (8, 24). Additional studies will be needed to better understand the nature and regulation of conformational changes that viral fusion class I proteins undergo to trigger membrane fusion.

ACKNOWLEDGMENTS

This work was partially supported by grants from Junta de Castilla y León (SA009A08) to I.M.-B. and from Fondo de Investigaciones Sanitarias (FIS) (PI08/1813) to E.V. J.A. is a predoctoral fellowship holder from the Spanish Ministerio de Educación, Cultura y Deportes (FPU program; AP-2004-6065).

We thank Adolfo García-Sastre for providing anti-HN and polyclonal anti-NDV. Thanks are also due to N. Skinner for language corrections.

REFERENCES

1. **Baker, K. A., R. E. Dutch, R. A. Lamb, and T. S. Jardetzky.** 1999. Structural basis for paramyxovirus-mediated membrane fusion. Mol. Cell **3:**309–319.
2. **Campbell, R. E., O. Tour, A. E. Palmer, P. A. Steinbach, G. S. Baird, D. A. Zacharias, and R. Y. Tsien.** 2002. A monomeric red fluorescent protein. Proc. Natl. Acad. Sci. USA **99:**7877–7882.
3. **Chen, L., J. J. Gorman, J. McKimm-Breschkin, L. J. Lawrence, P. A. Tulloch, B. J. Smith, P. M. Colman, and M. C. Lawrence.** 2001. The structure of the fusion glycoprotein of Newcastle disease virus suggests a novel paradigm for the molecular mechanism of membrane fusion. Structure **9:**255–266.
4. **Connolly, S. A., G. P. Leser, T. S. Jardetzky, and R. A. Lamb.** 2009. Bimolecular complementation of paramyxovirus fusion and hemagglutinin-neuraminidase proteins enhances fusion: implications for the mechanism of fusion triggering. J. Virol. **83:**10857–10868.
5. **Dutch, R. E., S. B. Joshi, and R. A. Lamb.** 1998. Membrane fusion promoted by increasing surface densities of the paramyxovirus F and HN proteins: comparison of fusion reactions mediated by simian virus 5 F, human parainfluenza virus type 3 F, and influenza virus HA. J. Virol. **72:**7745–7753.
6. **Dutch, R. E., T. S. Jardetzky, and R. A. Lamb.** 2000. Virus membrane fusion proteins: biological machines that undergo a metamorphosis. Biosci. Rep. **20:**597–612.
7. **Ferreira, L., I. Muñoz-Barroso, F. Marcos, V. L. Shnyrov, and E. Villar.** 2004. Sialidase, receptor-binding and fusion-promotion activities of Newcastle disease virus haemagglutinin-neuraminidase glycoprotein: a mutational and kinetic study. J. Gen. Virol. **85:**1981–1988.
8. **Gainey, M. D., M. J. Manuse, and G. D. Parks.** 2008. A hyperfusogenic F protein enhances the oncolytic potency of a paramyxovirus simian virus 5 P/V mutant without compromising sensitivity to type I interferon. J. Virol. **82:**9369–9380.
9. **Glaser, L., J. Stevens, D. Zamarin, I. A. Wilson, A. Garcia-Sastre, T. M. Tumpey, C. F. Basler, J. K. Taubenberger, and P. Palese.** 2005. A single amino acid substitution in 1918 influenza virus hemagglutinin changes receptor binding specificity. J. Virol. **79:**11533–11536.
10. **Lamb, R. A., and G. D. Parks.** 2007. Paramyxoviridae: the viruses and their replication, p. 1449–1496. *In* D. M. Knipe et al. (ed.), Fields virology, 5th ed., vol. 1. Lippincott Williams & Wilkins, Philadelphia, PA.
11. **Li, J., V. R. Melanson, A. M. Mirza, and R. M. Iorio.** 2005. Decreased dependence on receptor recognition for the fusion promotion activity of L289A-mutated Newcastle disease virus fusion protein correlates with a monoclonal antibody-detected conformational change. J. Virol. **79:**1180–1190.
12. **Luque, L. E., and C. J. Russell.** 2007. Spring-loaded heptad repeat residues regulate the expression and activation of paramyxovirus fusion protein. J. Virol. **81:**3130–3141.
13. **McGinnes, L. W., T. Sergel, H. Chen, L. Hamo, S. Schwertz, D. Li, and T. G. Morrison.** 2001. Mutational analysis of the membrane proximal heptad repeat of the Newcastle disease virus fusion protein. Virology **289:**343–352.
14. **Nakaya, T., J. Cros, M. S. Park, Y. Nakaya, H. Zheng, A. Sagrera, E. Villar, A. Garcia-Sastre, and P. Palese.** 2001. Recombinant Newcastle disease virus as a vaccine vector. J. Virol. **75:**11868–11873.
15. **Niwa, H., K. Yamamura, and J. Miyazaki.** 1991. Efficient selection for high-expression transfectants with a novel eukaryotic vector. Gene **108:**193–199.
16. **Paterson, R. G., C. J. Russell, and R. A. Lamb.** 2000. Fusion protein of the paramyxovirus SV5: destabilizing and stabilizing mutants of fusion activation. Virology **270:**17–30.
17. **Russell, C. J., T. S. Jardetzky, and R. A. Lamb.** 2001. Membrane fusion machines of paramyxoviruses: capture of intermediates of fusion. EMBO J. **20:**4024–4034.
18. **Russell, C. J., K. L. Kantor, T. S. Jardetzky, and R. A. Lamb.** 2003. A dual-functional paramyxovirus F protein regulatory switch segment: activation and membrane fusion. J. Cell Biol. **163:**363–374.
19. **Russell, C. J., and L. E. Luque.** 2006. The structural basis of paramyxovirus invasion. Trends Microbiol. **14:**243–246.
20. **San Román, K., E. Villar, and I. Muñoz-Barroso.** 1999. Acidic pH enhancement of the fusion of Newcastle disease virus with cultured cells. Virology **260:**329–341.
21. **Sergel, T. A., L. W. McGinnes, and T. G. Morrison.** 2000. A single amino acid change in the Newcastle disease virus fusion protein alters the requirement for HN protein in fusion. J. Virol. **74:**5101–5107.
22. **Sergel, T. A., L. W. McGinnes, and T. G. Morrison.** 2001. Mutations in the fusion peptide and adjacent heptad repeat inhibit folding or activity of the Newcastle disease virus fusion protein. J. Virol. **75:**7934–7943.
23. **Sergel-Germano, T., C. McQuain, and T. Morrison.** 1994. Mutations in the fusion peptide and heptad repeat regions of the Newcastle disease virus fusion protein block fusion. J. Virol. **68:**7654–7658.
24. **Vigil, A., M. S. Park, O. Martinez, M. A. Chua, S. Xiao, J. F. Cros, L. Martinez-Sobrido, S. L. Woo, and A. Garcia-Sastre.** 2007. Use of reverse genetics to enhance the oncolytic properties of Newcastle disease virus. Cancer Res. **67:**8285–8292.
25. **West, D. S., M. S. Sheehan, P. K. Segeleon, and R. E. Dutch.** 2005. Role of the simian virus 5 fusion protein N-terminal coiled-coil domain in folding and promotion of membrane fusion. J. Virol. **79:**1543–1551.
26. **Yin, H. S., R. G. Paterson, X. Wen, R. A. Lamb, and T. S. Jardetzky.** 2005. Structure of the uncleaved ectodomain of the paramyxovirus (hPIV3) fusion protein. Proc. Natl. Acad. Sci. USA **102:**9288–9293.
27. **Yin, H. S., X. Wen, R. G. Paterson, R. A. Lamb, and T. S. Jardetzky.** 2006. Structure of the parainfluenza virus 5 F protein in its metastable, prefusion conformation. Nature **439:**38–44.